Journal of the Korean Nuclear Society
Volume 23, Number 3, September 1991

An Investigation of Pressure Drop Characteristics of Finned Rod Bundles

Moo-Ki Chung, Chang-Hwan Chung, Heung-June Chung, Chul-Hwa Song, Sun-Kyu Yang

Korea Atomic Energy Research Institute

(Received January 17, 1991)

핀 봉다발의 압력강하 특성연구

정문기 · 정장환 · 정흥준 · 송철화 · 양선규

한국원자력연구소

(1991. 1. 17 접수)

Abstract

A multi-purpose research reactor called KMRR has been developed by Korea Atomic Energy Research Institute(KAERI) to generate a maximum thermal output of 30 MW. As a part of thermal hydraulics study, pressure drop characteristics of the longitudinally finned fuel rod bundles were experimentally investigated in a recirculating water test loop. The present study is focused on the investigation of fin effects on pressure drop and the development of pressure drop correlation for the finned rod bundles in a wide range of flow conditions. Friction factor correlations for each design of the finned rod bundles are developed. The value of friction factor for the finned rod bundles was higher than the analytical solution (64/Re) of laminar circular channel flow but became lower than the Blasius equation as Reynolds number was increased.

요 약

30 MW 열출력을 갖는 다목적 연구용 원자로(KMRR)가 원자력연구소에서 개발되고 있다. 열수력 연구의 일환으로 길이 방향으로 핀이 달린 연료봉다발의 압력강하특성을 실험으로 연구하였다. 본 논문에서는 넓은 유량범위에서 적용할 수 있는 핀 연료봉다발에서의 압력강하 상관식의 도출과 압력강하에 미치는 핀 영향의 조사에 중점을 두었다. 도출된 KMRR 핵연료 봉다발의 마찰계수 상관식을 원형관의 실험결과와 비교하였을 때 저유량 실험영역에서는 층류시의 해석값인 64/Re 보다 큰 값을 가졌으나 Re가 증가되면 Blasius 상관식보다 낮아지는 경향을 나타내었다.

1. Introduction

Korea Multi-purpose Research Reactor(KMRR) has been developed by Korea Atomic Energy Research Institute. It is upward-flowing, light-water cooled reactor with an open-chimney-in-pool arrangement. The reactor core consists of 36-rod driver fuel bundles and 18-rod shim fuel bundles. Because the linear heat generation rate of the fuel rods is remarkably high, longitudinal fins are provided on the fuel element surfaces to enhance removal of this excessive heat. Thus the fuel bundles are characterized by the presence of a num-

ber of longitudinal fins on the surfaces of fuel rods. The fuel bundles are normally cooled by the upward axial flow circulated by the reactor pumps. In accident conditions, they are cooled under natural convection mode.

Rheme [1,2], Deissler and Taylor [3] studied pressure drop along the bare rod bundles in triangular and square lattices with different pitch to diameter ratio. They represented friction factor correlations for the bare rod bundles. In spite of numerous previous pressure drop studies, very little information is available on longitudinally finned rod bundles. Grover and Venkat Raj [4] performed pressure drop measurements on the 7-rod bundles with 3 longitudinal fins per each rod and the pitch to equivalent rod diameter ratios of about 1.03 and 0.95.

The pressure drop characteristics for the finned rod bundles in a wide range of flow velocity is essential in the evaluation of the performance of the KMRR fuels in steady state as well as transient conditions. As a part of the fuel design and safety analysis activity for the reactor, pressure drop characteristics of several designs of the fuel bundles are experimentally investigated in a flow test loop in KAERI [5]. This paper discusses details of the experiments and the effects of the longitudinal fins on pressure drop characteristics in a wide range of flow velocity.

2. Types of Rod Bundles

A rod bundle consists of a number of finned rods, bottom and top end plates, a central tie rod, and a flow resister. The finned rods are made of aluminium and each rod has equi-spaced longitu-

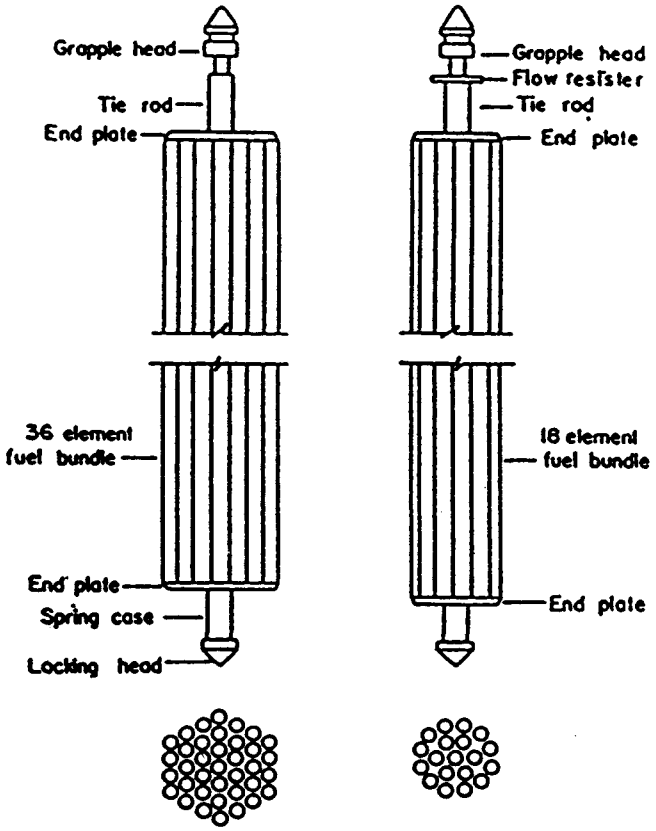

Fig. 1 Schematic of rod bundles

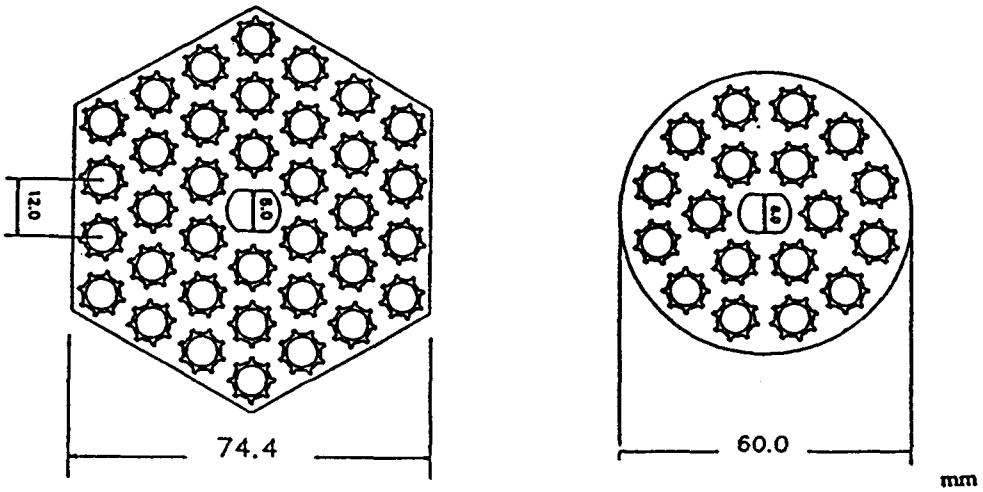

Fig. 2 Cross Section of Two Types of 8–Finned Rod Bundles

dinal fins on its surface. Configuration of the rod bundles is determined by the end plates locating at each end of the rods. Two types of the standard rod bundle, i.e., 8–finned 36–rod bundle and 8–finned 18–rod bundle, are shown in Figure 1. The 36–rod bundle is arranged in hexagonal geometry, and the shape of the subchannels determined by the rods are triangular. The 18–rod bundle is arranged in circular geometry, and the subchannels are mixed with triangular and square types Figure 2 shows the cross section of the rod bundles installed in the test section of the cold test loop. A flow resister is attached on the top of the rod bundles, and it is intended to give additional flow resistance to the bundle. To investigate the effects of fin on pressure drop, additional test bundles are made by changing the number of the rod fins from 8 to 6, or by orienting the rod fin regularly or randomly. Details for the finned rod bundles under investigations are listed in Tables 1 and 2.

3. Experimental Setup

A schematic diagram of the test loop is shown in Figure 3. The loop consists of two pumps, a vertical test section, and a water storage tank. Inventory of the storage tank is made large to give

Table 1 Parameters of Finned Rods

Parameter	8–Finned rod	6–Finned rod
Length of rod	766mm	
Dia. of rod	8.87mm	
Fin height	1.02mm	
Fin width	0.76mm	
Number of fin	8ea	6ea
Perimeter of a rod	41.04mm	36.96mm
Equi. rod dia.	13.06mm	11.76mm
Pitch/equi. dia.	0.92	1.02

Table 2 Hydraulic Parameters of Rod Bundles

Rod bundle		Hydraulic dia.(mm)	Wetted perimeter(mm)	Flow area (mm^2)
18–rod bundle	8 fin	7.3565	959.33	1764.33
	6 fin	8.0923	885.89	1792.24
36–rod bundle	8 fin	6.2091	176.36	2743.42
	6 fin	6.9096	1620.48	2799.23

constant water temperature during the experiment. Two pumps, a small one and a big one, are installed in parallel and pump operation is switched according to the desired test flow rate. Flow rate is controlled by two globe valves installed downstream of each pump. The test section consists of the rod bundle enclosed in a transparent acrylic tube with the same shapes, hexagonal or circular, of rod bundles. The acrylic tube allows visual observation of the rod bundle during the flow test.

Differential pressure is measured across the orifices installed on 2″ and 4″ pipings upstream of the test section, and the flow rate corresponding to the measured differential pressure is calculated from the orifice equation of the ASME fluid meters [6]. The test section is instrumented for the measurements of temperature, pressure, and pressure drop across the components of rod bundle. Water temperature is measured with a K-type thermocouple. Loop pressure is measured with a capacitance type pressure transmitter installed at the inlet of the test section. Pressure taps are located across end plates and flow resister as well as the clear length of the rod bundle. And pressure drops across the tap pairs are measured with 5 D/P transmitters with different measuring ranges.

The analog signals from the instruments are gathered with a HP 3054A data acquisition system and tranferred to a micro-computer connected to a plotter and a printer. Following this, thermodynamic properties, flow rate, Reynolds number, friction factor and minor loss coefficients of the rod bundle are calculated with the computer, and the results are displayed on the computer peripherals.

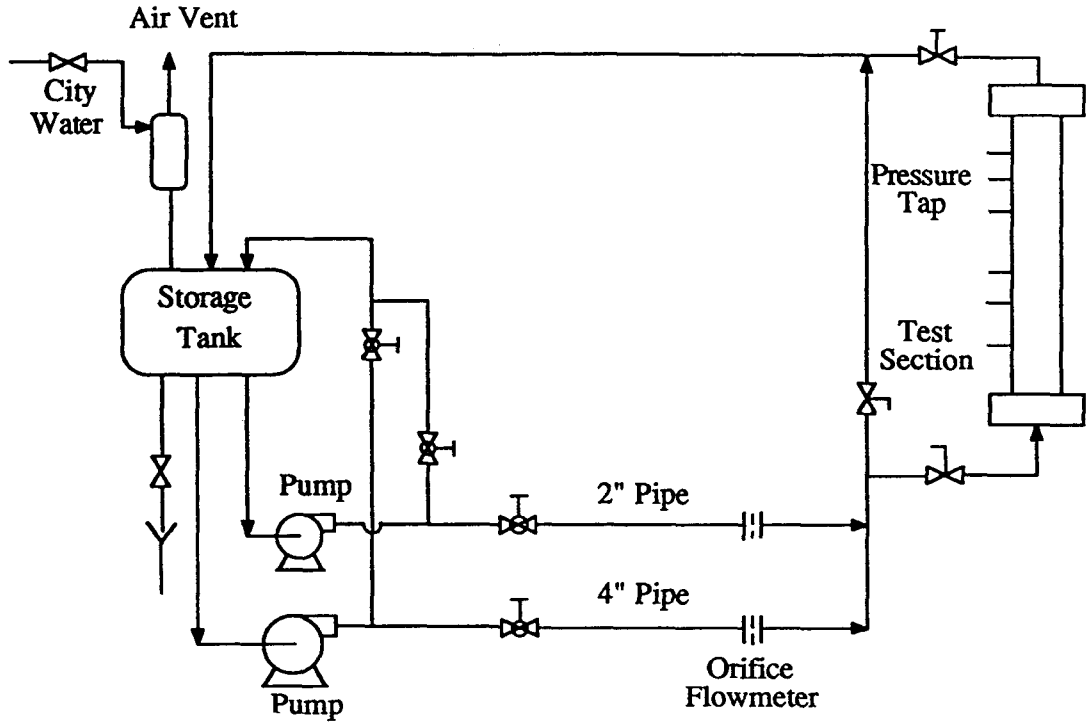

Fig. 3 Flow Diagram of Cold Test Loop

4. Experiments

Before the experiments, the loop is filled with water and the pump is operated to raise water temperature to the desired temperature. The experimental conditions for each type of rod bundles are listed in Table 3. Water temperature is maintained at 30℃ or 40℃. The pressure at the test section inlet is measured to be in the range of 0.1~2.0 bars according to the flow impedance of the rod bundle in the test section. Flow rate is measured with one of the orifice flow meters on the parallel pipings upstream of the test section. The small orifice meter is used for flow rate of 0.2~2.5kg/s, and the large meter for 2.5~24kg/s. Pressure drops across each component of the rod bundle are measured according to the test matrix in Table 3.

Table 3 Pressure Drop Test Matrix

Rod bundle		Fin array	Number of test	Flow rate	Temp.
18-rod bundle	8 fin	Random	62	0.2~16 kg/sec	30℃ or 40℃
		Regular	60		
	6 fin	Regular	54		
36-rod bundle	8 fin	Random	58	0.2~24 kg/sec	
		Regular	56		
	6 fin	Regular	57		

5. Results and Discussions

5.1 Pressure Drop along Rod Bundle

The pressure drop of the rod bundle can be considered to be composed of frictional pressure loss along the bundle and minor loss across its components. In this experiment, pressure drops are measured across locking head, bottom end plate, clear length of the finned rod, top end plate, and grapple head as shown in Figure 4.

Figure 5 shows typical results of the measured differential pressure as a function of flow rate for the 8-finned 18-rod bundle. It is noted that large parts of the total pressure drop occured by frictional pressure loss along the clear length of the finned rod bundle. Pressure drops of top end plate and bottom end plate are smaller than the frictional pressure loss. Although pressure drops for locking head and grapple head are not displayed on the figure, they are measured to be negligible compared to those of other components. The bottom end plate produces more appa-

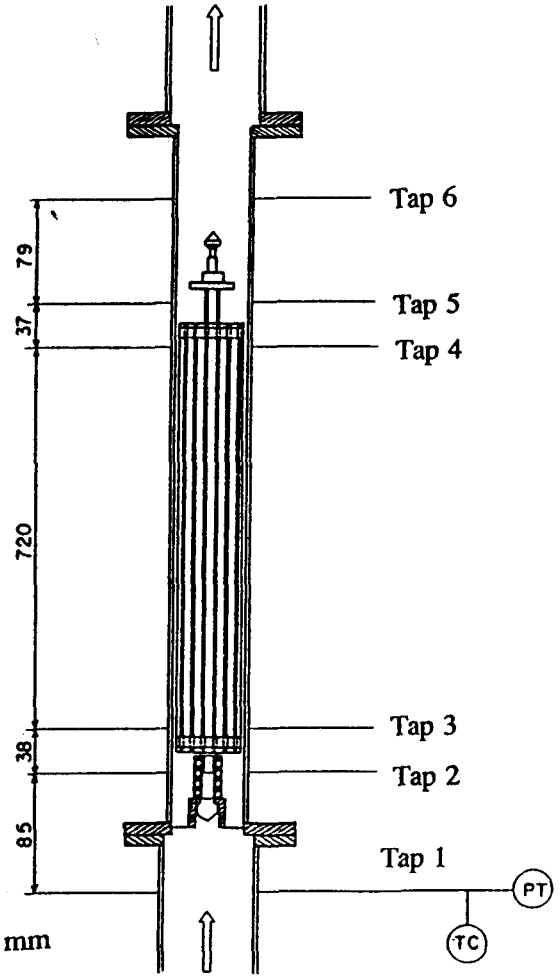

Fig. 4 Location of Pressure Taps

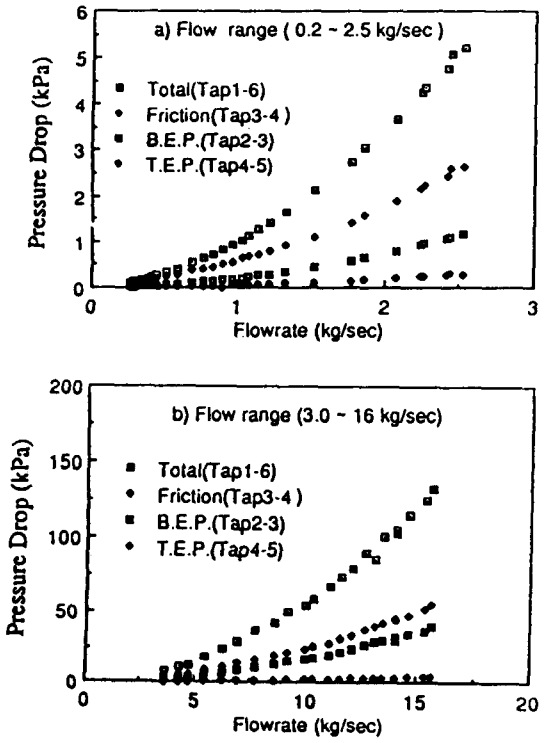

Fig. 5 Pressure Drop vs. Flow Rate for 8–Finned 18–Rod Bundle

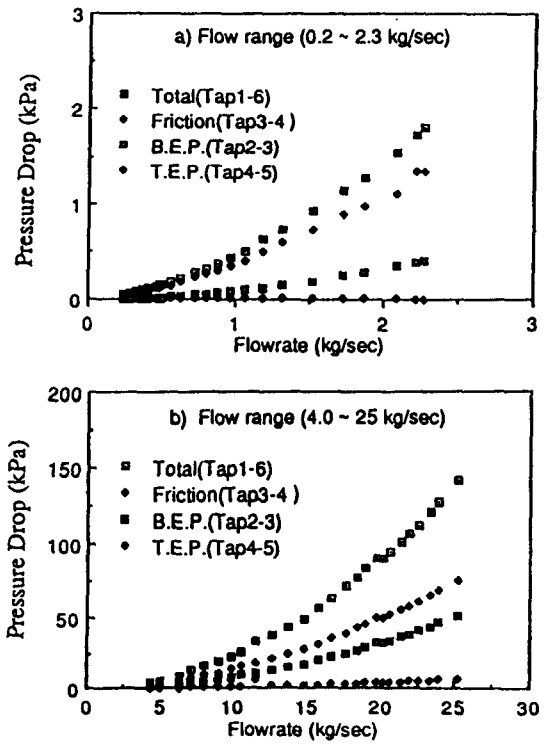

Fig. 6 Pressure Drop vs. Flow Rate for 8–Finned 36-Rod Bundle

rent pressure drop than the top end plate because the upstream pressure tap for the bottom end plate is located at a lower flow velocity region than the downstream pressure tap. When the area change is considered in the calculation of the pressure loss, the top end plate produced a little more pressure loss than the bottom end plate due to the high turbulence occuring behind the top end plate.

The measured differential pressure for the 8–finned 36–rod bundle is shown in Figure 6. The pressure drop attribution of the components of the rod bundle is similar to that of the above mentioned 18–rod bundle.

5–2. Frictional Pressure Loss

Pressure drop data measured along the clear length of a rod bundle are used to determine the value of friction factor for the finned rod bundle. The friction factor f is calculated from the following Darcy–Weisbach equation:

$$\Delta P = f \frac{L}{D_h} \frac{\rho V^2}{2}$$

The "equivalent hydraulic diameter"(D_h) for the rod bundles is obtained by $D_h = 4A/P_e$. A is the flow area of the rod bundle, and P_e is total length of the wetted periphery of the flow tube and finned rods at the bundle cross section. The calculated friction factors are plotted against the Reynolds numbers, and also compared with the Blasius equation for smooth tube as well as the analytical solution for laminar circular channel flow. Pressure loss along bare rod bundles has been generally predicted by assuming similarity to that for flow inside a tube and by using the equivalent hydraulic diameter concept. The valid-

ity of using the equivalent hydraulic diameter concept in the prediction of pressure drop in a bare rod bundle was investigated by Deissler and Taylor. They observed that pressure drop characteristics of bare rod bundles are varied as a function of pitch to diameter ratio, and that friction factor for a bare rod bundle with triangular array at p/d=1.0 is about 55% of that of the circular channel.

Grover et al. defined the "equivalent rod diameter" in their study so that an unfinned rod having a diameter equal to the equivalent rod diameter will have the same perimeter as the finned rod. Equivalent rod diameters, as defined above, for every type of the rod bundles tested in this experiment are given in Table 1 and 2. It is noted that the values of pitch to equivalent rod diameter ratio (p/d_e) for every type of the rod bundles are about 1.0.

Skin friction factor due to wall shear for the 8-finned 18-rod bundle is shown in Figure 7. The test flow covers Reynolds numbers from 1,200 to 100,000 in which laminar, transition, and turbulent flow modes can be observed in the flow of a circular channel. The friction factor decreases gradually as the Reynolds number increases, and the scatter of friction factor which is expected in the transition flow region has not been observed. Compared to the friction factor (f=64/Re) of a laminar tube flow and the Blasius equation applicable to a turbulent tube flow, the test results are higher than 64/Re and slightly lower than the

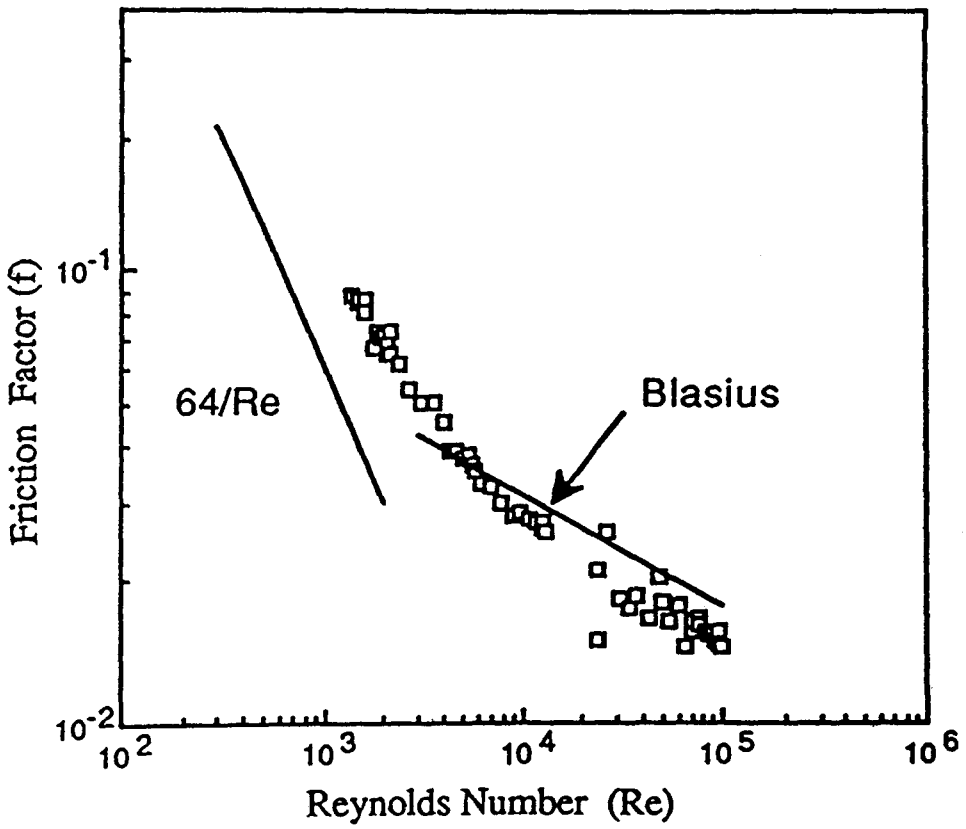

Fig. 7 Friction Factor for 8-Finned 18-Rod Bundle

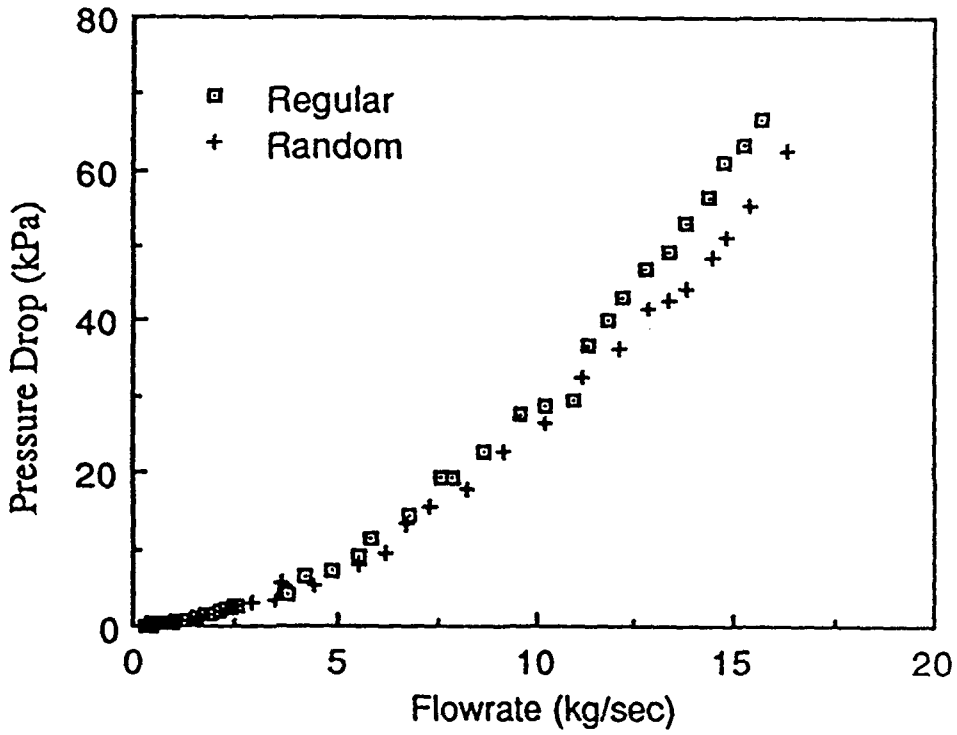

Fig. 8 Comparison of Pressure Loss for 8-Finned 18-Rod Bundles Having Different Fin Orientation

Blasius equation in the corresponding flow ranges.

Figure 8 compares pressure losses of the 8-finned 18-rod bundles for the two types of fin orientation ; one test bundle is assembled so that rod fins are oriented regularly as shown in Figure 2, and the other is oriented randomly. Pressure loss of the regularly orinented bundle becomes greater than that of the randomly oriented as flow rate is increased.

Figure 9 shows the friction factor of 8-finned and 6-finned 18-rod bundles. The friction factor of the 6-finned bundle is a little higher than that of the 8-finned bundle. From the test results, it can be said that the longitudinal fins have some effects on pressure drop such that the values of the friction factor are decreased as the number of fin is increased from 6 to 8.

The friction factor of the 8-finned 36-rod bundle is shown in Figure 10. The friction factor decreases logarithmically in the test flow range. The experimental results are higher than $64/Re$ at low flow velocity and lower than the Blasius equation at high flow velocity. Figure 11 shows the effects of fin orientation on pressure loss for 8-finned 36-rod bundle. Because the two cases of the bundle orientation produce almost the same values of friction loss, the fin orientation effects are negligible in this bundle geometry. It is also noted that the fin orientation effects are shown only in the 18-rod bundles having two types of subchannels, i.e., square and triangular subchannels. Figure 12 compares friction factors for 8-finned and 6-finned 36-rod bundles. The 6-finned bundle produces a little higher friction factor than the 8-finned bundle. Friction factor correlation for each type of the rod bundles has been developed

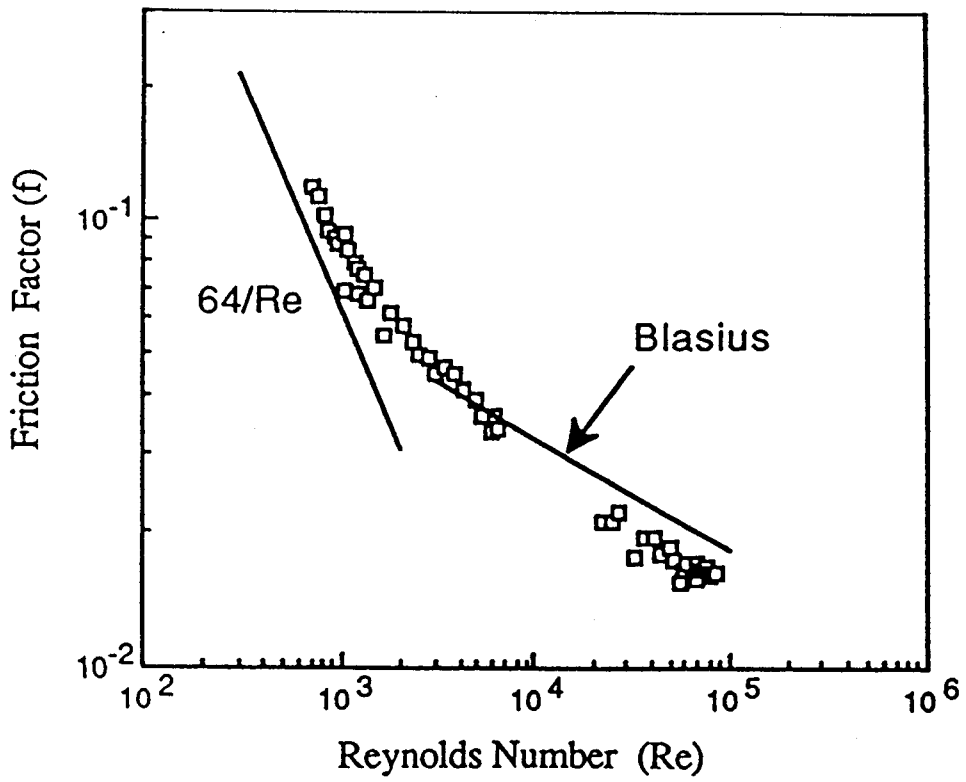

Fig.9 Comparison of Friction Factor for 6-Finned and 8-Finned 18-Rod Bundles

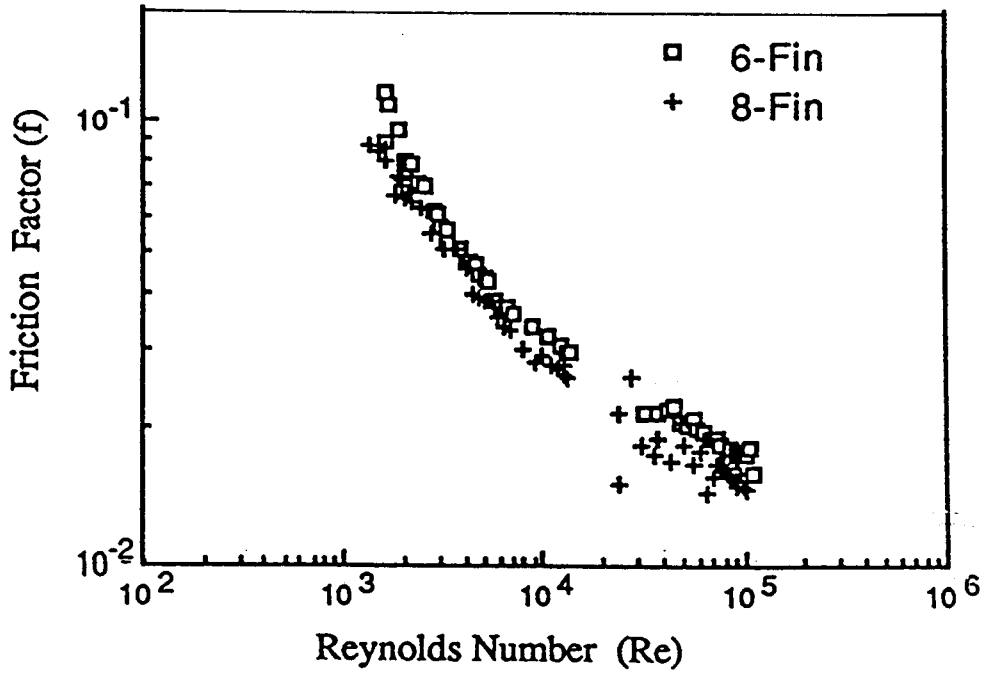

Fig. 10 Friction Factor for 8-Finned 36-Rod Bundle

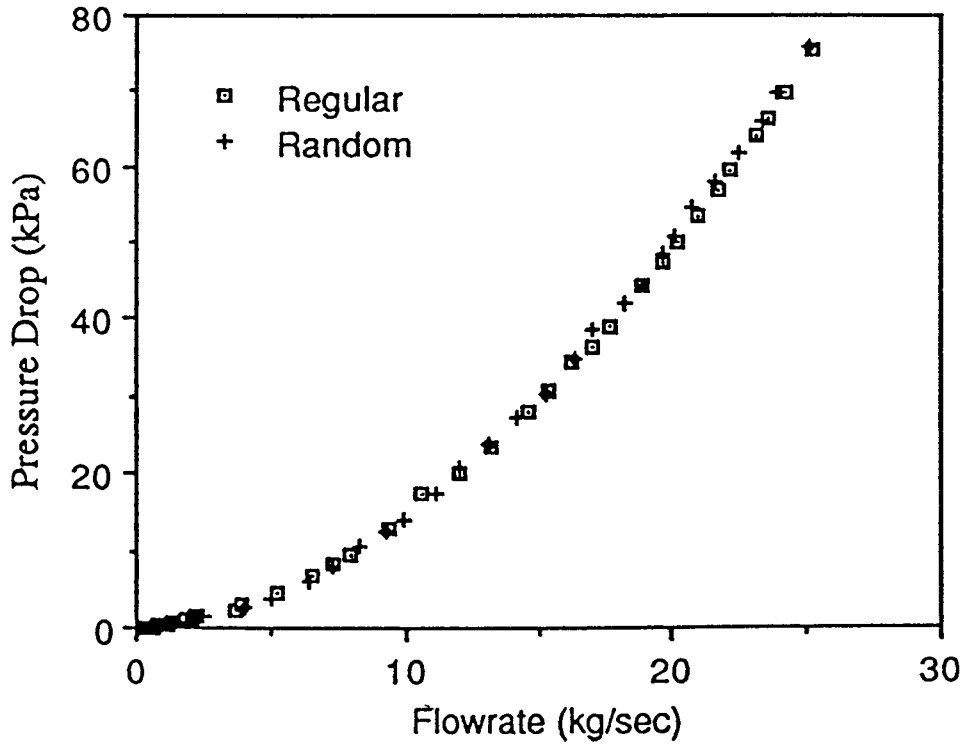

Fig. 11 Comparison of Pressure Loss for 8-Finned 36-Rod Bundles Having Different Fin Orientation

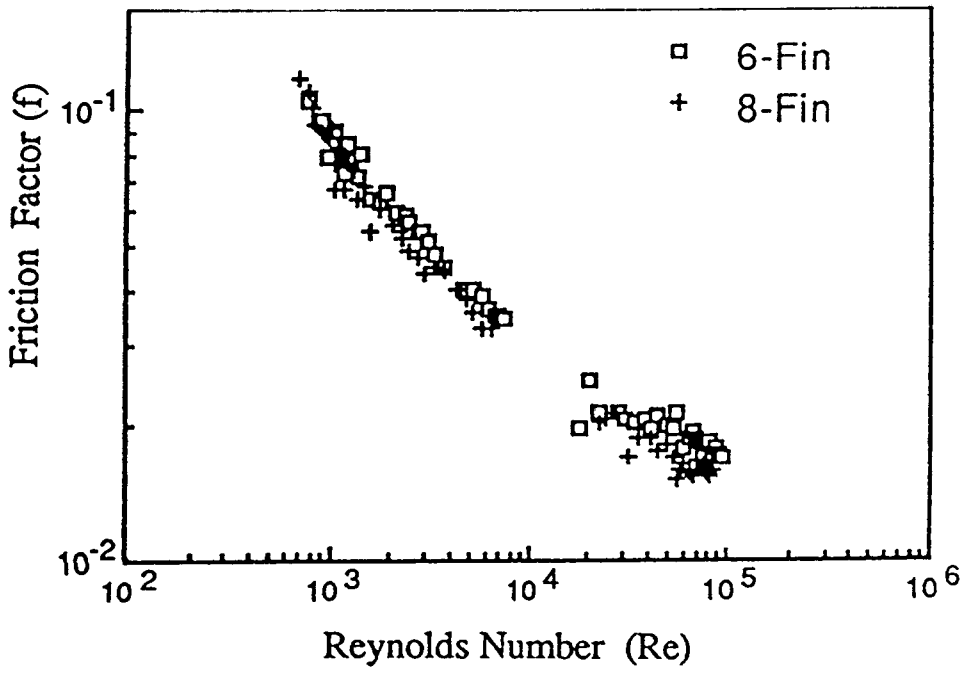

Fig. 12 Comparison of Friction Factor for 6-Finned and 8-Finned 36-Rod Bundles

Table 4 Friction Factor Correlations for the Finned Rod Bundles with Regular Fin Orientation

Rod bundle		Friction factor correlation	Reynolds number
18-rod bundle	8 fin	$f=1.38\ Re^{-0.41}$	$1.3\times10^3\leq Re\leq1.0\times10^5$
	6 fin	$f=1.31\ Re^{-0.38}$	$1.5\times10^3\leq Re\leq1.0\times10^5$
36-rod bundle	8 fin	$f=1.15\ Re^{-0.39}$	$7.0\times10^2\leq Re\leq1.0\times10^5$
	6 fin	$f=0.93\ Re^{-0.36}$	$7.0\times10^2\leq Re\leq1.0\times10^5$

by a least-square-fit method and listed in Table 4. The error of the correlation is within 3% in the entire range of the measurement.

A comparison of the friction factors for all types of finned rod bundles is made in Figure 13. The friction factors of the 6-finned rod bundles are higher than those of the 8-finned rod bundles. From the test results, it can be said that the effect of p/d_e is shown in the finned rod bundles like as that of p/d in bare rod bundles. For finned rod bundles, the value of p/d_e is related to the fin number in applying the equivalent rod diameter concept. And for every type of the rod bundles

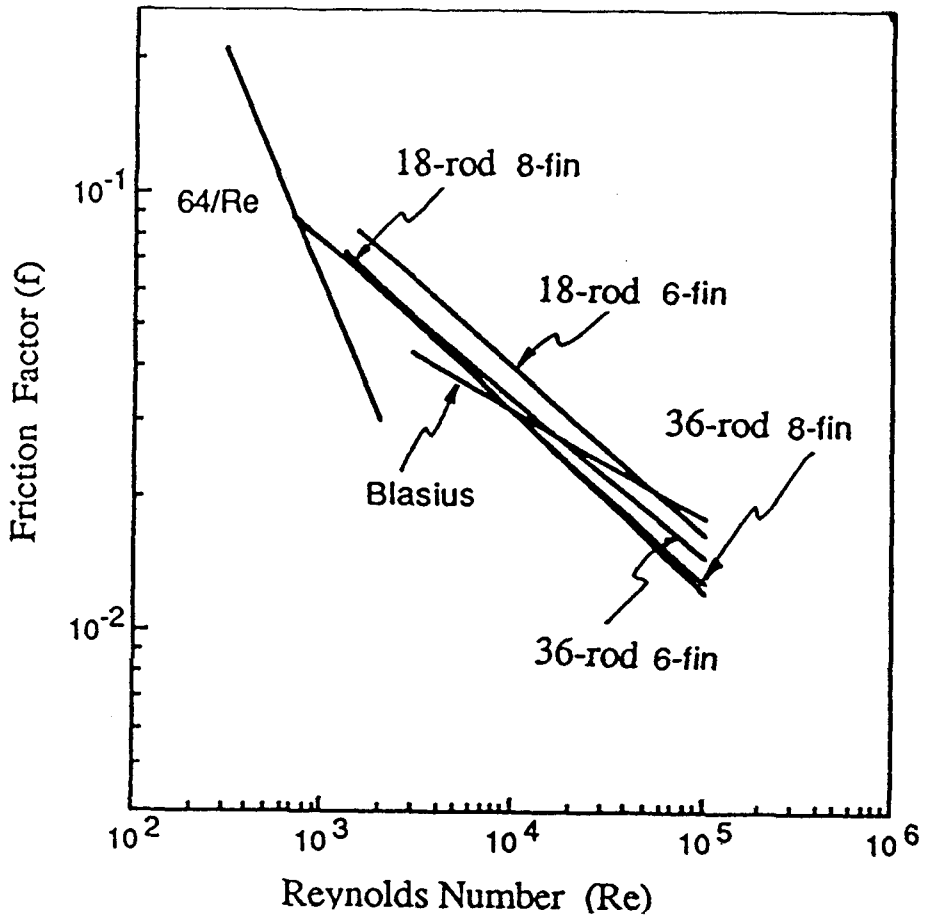

Fig. 13 Comparison of Friction Factor Correlations for the Finned Rod Bundles with Regular Fin Orientation

friction factors are greater than the Blasius equation in the low Reynolds number region but they become smaller than the Blasius equation in high Reynolds number region. The experimental results are not in line with the observation of other investigators that the friction factor for bare rod bundless with p/d 1.08 is less than that for smooth circular tube and the friction factor for the bare rod bundles with triangular array at p/d=1.0 amounts to 55% of the values of circular channel friction factor. Bare rod bundles with p/d=1.0 can not have cross flow between adjacent subchannels which results in no momentum exchange between them. But the rod bundles tested here have some gaps among adjacent rods although p/d_e of the rod bundles is less than 1.0. As previously mentioned, Grover compared the friction factor of finned rod bundles with that for smooth tubes on the basis of p/d_e. And he demonstrated that the equivalent rod diameter concept is appropriate for the 3–finned 7–rod clusters having $p/d_e \sim 1.03$ and 0.95 in their test flow range. For the currently tested 18 or 36–rod bundles composed of 6 or 8–finned rods, the test results were different from those of Grover et.al. The friction factor evaluated by using equivalent rod diameter concept did not show the same trend of the Blasius equation and that of bare rod bundles over a wide range of flow velocity.

6. Conclusions

Hydraulic tests with several designs of the finned rod bundles have been carried out to investigate their pressure drop characteristics in a wide range of flow conditions. Friction factor correlations are developed for each type of the finned rod bundles and compared with other studies of circular channels and bare rod bundles.

The friction factor for the finned rod bundles was gradually decreased from low flow velocity (Re~600) to relatively high velocity ($Re \sim 1 \times 10^5$). And the scatter of friction factor which is representative in transition flow was not observed in the test flow conditions. The friction factor was greater than the analytical solution for laminar circular channel flow in the tested flow range, but the friction factor became smaller than the Blasius equation as Reynolds number is increased.

The friction factor for the finned rod bundles evaluated by using equivalent rod diameter showed the general pressure loss tendency of bare rod bundles only in high Reynolds number region. Thus, the applicability of the equivalent diameter concept should be validated in the estimation of pressure drop of finned rod bundles by using the test data of bare rod bundles.

References

1. K. Rheme, Pressure Drop Performance of Rod Bundles in Hexagonal Arrangements, Int. J. Heat Mass Transfer, Vol. 15, pp. 24–99, 1972
2. K. Rheme, Simple Method of Predicting Friction Factors of Turbulent Flow in Non–circular Channels, Int. J. Heat Mass Transfer, Vol. 16, pp. 933–950, 1973
3. R. G. Deissler and M. F. Taylor, Analysis of Axial Turbulent Flow and Heat Transfer through Banks of Rods and Tubes, Proc. Reactor Heat Transfer Conf., Part 1, Book 2, p. 416, TID–7529, USAEC, 1957
4. R. B. Grover and V. Venkat Raj, Pressure Drop along Longitudinally–finned Seven–rod Cluster Nuclear Fuel Elements, Nuclear Engineering and Design, Vol. 58, pp. 79–83, 1980
5. M. K. Chung et al., "Fluid Flow Test for KMRR Fuel Assemblies", KAERI/RR–839/89, 1989
6. Howard S. Bean, Fluid Meters ; Their Theory and Application, ASME, 1971